

A network-of-networks model for physical networks

Gábor Pete,^{1,2} Ádám Timár,^{1,3} Sigurdur Örn Stefánsson,³ Ivan Bonamassa,⁴ and Márton Pósfai^{4,*}

¹*Alfréd Rényi Institute of Mathematics, Budapest, Hungary*

²*Budapest University of Technology and Economics, Budapest, Hungary*

³*University of Iceland, Reykjavík, Iceland*

⁴*Department of Network and Data Science, Central European University, Vienna, Austria*

(Dated: June 5, 2023)

Physical networks are made of nodes and links that are physical objects embedded in a geometric space. Understanding how the mutual volume exclusion between these elements affects the structure and function of physical networks calls for a suitable generalization of network theory. Here, we introduce a network-of-networks framework where we describe the shape of each extended physical node as a network embedded in space and these networks are bound together by physical links. Relying on this representation, we model the growth of physical networks, showing for a general class of systems that volume exclusion induces heterogeneity in both node volume and degree, with the two becoming correlated. These emergent structural properties strongly affect the dynamics on physical networks: by calculating their Laplacian spectrum as a function of the coupling strength between the nodes we show that volume-degree correlations suppress the tail of the spectrum. Finally, we apply our theoretical framework to a large-scale three-dimensional map of a fruit fly brain, finding analog behavior with the networks generated by our growth model.

INTRODUCTION

The building blocks of physical networks are extended objects that do not intersect each other, resulting in non-trivial geometric layouts [1], link entanglement [2] and emergent correlations between physical and network structure [3]. Yet, these works model nodes as localized spheres connected by extended tube-like links, an assumption that does not necessarily reflect the structure of most real-world physical networks. In the connectome, for example, nodes represent neurons with non-trivial dendritic shapes and links are point-like synapses [4]. A similar picture emerges for molecular networks such as the cytoskeleton, mitochondrial networks or fiber materials, where nodes are extended molecular strands and bonds between them are localized [5–7], as well as in the wood-wide-web, where extended tree roots and mycelia connect to form a complex underground network [8, 9]. Therefore, the sphere-tube paradigm often falls short at describing physical networks, calling for a more general framework to cope with the complex shape of nodes and links.

In this work we develop a network-of-networks representation of physical networks that is able to capture arbitrary node shapes [10, 11] and allows us to characterize both structural and dynamical properties of networks. Relying on the network-of-networks framework, we introduce a model that grows physical networks from fractal segments. Analytically solving the model, we show that physicality induces heterogeneity in both the physical and the network properties of the nodes and that the two become strongly correlated. These correlations also affect the dynamics on the networks: generalizing the combinatorial Laplacian to physical networks [12–14], we show that fast dynamical modes associated to hubs (and

corresponding to the tail of the Laplacian spectra) are suppressed by the emergent correlations between node volume and degree. The usefulness of the mathematical tools we develop in this paper go beyond the specifics of the model, and we demonstrate this by applying our framework to a recently collected data set describing more than $\sim 20,000$ neurons of a fruit fly’s brain [15]. In doing so, we identify structural correlations similar to correlations in our physical network growth model, and we show that these have an analog effect on the Laplacian spectrum of the connectome.

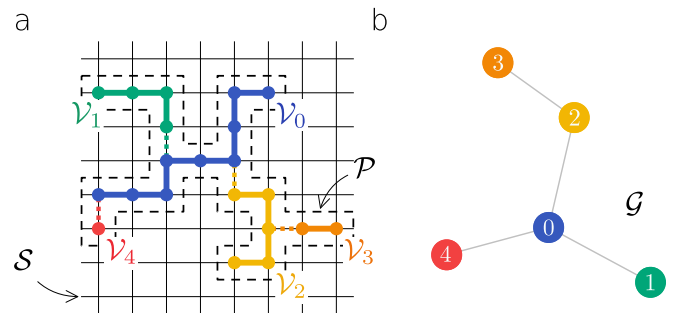


FIG. 1. **Network-of-networks representation.** (a) Each physical node \mathcal{V}_i is a subgraph of the substrate \mathcal{S} . Physical nodes cannot overlap, i.e., $\mathcal{V}_i \cap \mathcal{V}_j = \emptyset$ for $i \neq j$. The physical layout \mathcal{P} (dashed area) is a network-of-networks: it is the union of physical nodes \mathcal{V}_i together with the bonds connecting them. (b) The combinatorial network \mathcal{G} is a coarse-grained representation of \mathcal{P} capturing the connections between the nodes without the physical structure.

NETWORK-OF-NETWORKS REPRESENTATION

We aim to describe physical networks embedded in some substrate or medium. In its most general form, the substrate is represented by a graph \mathcal{S} , and each physical node i is an extended object occupying a subgraph $\mathcal{V}_i \subset \mathcal{S}$. To capture volume exclusion, we do not allow nodes to overlap, i.e., $\mathcal{V}_i \cap \mathcal{V}_j = \emptyset$ for $i \neq j$. Two nodes i and j may form a link (i, j) if they occupy adjacent sites in \mathcal{S} . The physical layout \mathcal{P} of the network is a network-of-networks, i.e., it is the union of physical nodes, where each node is a network itself, together with the bonds forming the connections between the nodes (Fig. 1a). The layout \mathcal{P} is a physical realization of the combinatorial network, \mathcal{G} , where node i of \mathcal{G} corresponds to the physical node \mathcal{V}_i , and nodes i and j are connected if there is a bond between \mathcal{V}_i and \mathcal{V}_j in \mathcal{P} (Fig. 1b). Though the substrate \mathcal{S} can represent any available space, here we focus on substrates that are d dimensional cubic lattices with linear size L and periodic boundary conditions. Note that network representations of this kind are employed in the graph drawing literature with the focus on algorithms that embed a given combinatorial network into \mathcal{S} [16]. Here, we are interested in physical networks \mathcal{P} growing in \mathcal{S} , the emergent relation between \mathcal{P} and \mathcal{G} , and its consequences on the dynamics on the network.

NETWORK GROWTH

To study the effect of physicality on network evolution, we define a model of network growth relying on the network-of-networks representation. We start with an empty \mathcal{S} and we place a single node \mathcal{V}_0 occupying a subset of the sites. We add the rest of the nodes iteratively: At time step t we add a new node \mathcal{V}_t that is seeded at a random unoccupied site and grows until it hits an already existing node \mathcal{V}_s and a link $(t-s)$ is formed. The growth of node \mathcal{V}_t can be driven by any random or deterministic process; all that we assume is that each physical node is characterized by a fractal dimension $d_f \in [1, d]$ [17, 18]. We add N physical nodes or until all of \mathcal{S} is occupied; in the latter case we call the physical network saturated.

Since the total volume of the network increases over time, later nodes hit the network at higher rates and the typical size of nodes decreases. Hence, we expect that nodes added early have higher degree than nodes added in the final stages of the network evolution, both because they are larger and they have more time to collect connections. This suggests that to analytically characterize the evolution of the physical network two ingredients have to be considered: (i) *network growth*, i.e., nodes are added sequentially to the system and (ii) *externally limited* node growth, i.e., the nodes grow until they hit the already existing network. We show that these two ingredients lead

to the emergence of power law combinatorial networks with degree exponents $\gamma \leq 3$.

We start the analytical treatment of the model by estimating the probability p_{ij} that two randomly placed physical nodes \mathcal{V}_i and \mathcal{V}_j intersect. If the two boxes containing the physical nodes have side length $l_i \gg l_j$, respectively, and the larger node \mathcal{V}_i intersects the box containing the smaller node \mathcal{V}_j , then, by dimension counting, the two nodes overlap with positive probability if $d_f \geq d/2$. We can tile the lattice with $(L/l_j)^d$ boxes with side length l_j , and the number of such boxes intersected by \mathcal{V}_i is $\sim (l_i/l_j)^{d_f}$. Therefore the intersection probability is

$$p_{ij} \sim \frac{l_i^{d_f} l_j^{d-d_f}}{L^d} \sim \frac{v_i v_j^{d/d_f-1}}{L^d}, \quad (1)$$

where $v_i = |\mathcal{V}_i| \sim l_i^{d_f}$ is the volume of node i . If, however, $d_f < d/2$ and $l_j \leq l_i \ll L$, then the nodes avoid each other with high probability. In this case, the intersection probability will have the meanfield behavior, well-approximated by the probability of selecting the sites of \mathcal{V}_i and \mathcal{V}_j uniformly from \mathcal{S} , i.e., $p_{ij}^{\text{MF}} \sim v_i v_j / L^d$, which is independent of d_f and agrees with Eq. (1) for $d_f = d/2$.

Using the same box-counting argument that led to Eq. (1), the probability that a node added at time t intersects any existing node $s < t$ is approximately given by $\sum_{s < t} p_{st} = v_t^{d/d_f-1} V_{t-1} / L^d$, where V_{t-1} is the total volume of nodes $s < t$. A key observation is that the size of node t increases until it hits the existing network, meaning that v_t increases until $\sum_{s < t} p_{st} \approx 1$, allowing us to estimate the volume of node t as

$$v_t \approx (V_{t-1} / L^d)^{-\frac{d_f}{d-d_f}}. \quad (2)$$

Equation (2) allows us to express the evolution of the expected total volume via the recursion $V_{t+1} = v_{t+1} + V_t$ with initial condition $V_0 = v_0$. Using a continuous time approximation, we obtain

$$V_t \approx L^d \left[\frac{d}{d-d_f} \frac{t+c}{L^d} \right]^{\frac{d-d_f}{d}} \sim L^d \left(\frac{t}{L^d} \right)^{1-d_f/d}, \quad (3)$$

where c is a constant depending on v_0 . A natural choice for the latter is that the first node spans the entire available space, i.e., $v_0 \sim L^{d_f}$, in which case c is independent of L . Equation (3) predicts that N_{sat} , the number of nodes when the network saturates, scales as $N_{\text{sat}} \sim L^d$. As a consequence, for saturated networks, the physical layout \mathcal{P} is an asymptotically optimal embedding of the combinatorial network \mathcal{G} in the sense that there is no physical representation of \mathcal{G} that fits into smaller volume than $\sim L^d$.

In light of Eq. (3), we can now calculate the expected degree of the physical nodes in the combinatorial network \mathcal{G} . The time derivative of V_t shows that the volume of newly added nodes decreases as $v_t \sim (t/L^d)^{-d_f/d}$. Hence,

following Eq. (1), the expected degree of node t after the addition of N nodes is

$$k_t(N) = 1 + \frac{v_t}{L^d} \sum_{s=t+1}^N v_s^{d/d_f-1} \sim v_t \cdot \left(\frac{N}{L^d}\right)^{\frac{d}{d_f}}, \quad (4)$$

where the proportionality is valid for $t \ll N$. This means that the volume occupied by large nodes (i.e., nodes that were added early) in the physical layout is proportional to their degree in the combinatorial network.

We finally calculate the complementary cumulative degree distribution $P(k) = 1 - \frac{1}{N} \sum_{t:k_t \geq k}^N 1$, finding that $P(k) \sim k^{-(\gamma-1)}$ with exponent

$$\gamma = 1 + \frac{d}{d_f}, \quad (5)$$

For $d_f \leq d < 2d_f$ the degree exponent falls in the range $2 \leq \gamma < 3$. In the mean-field regime the degree exponent can be obtained by substituting d/d_f with 2, yielding $\gamma_{\text{MF}} = 3$. Note that the upper critical dimension of the physical network depends on the kinetic growth of the nodes. For example, growing nodes along a straight trajectory in a random direction generates nodes with $d_f = 1$; therefore the networks fall in the mean-field regime $d_f \leq d/2$ even for embedding dimension $d = 2$.

NUMERICAL SIMULATIONS

To test our analytical predictions, we numerically generate physical networks where nodes grow according to random walk trajectories. Specifically, we generate nodes using loop-erased random walks (LERWs), i.e., a trajectory that evolves as a simple random walk in which any loop is erased as soon as it is formed [19–22]. The LERW represents a tractable model of non-self-intersecting random trajectories. Its critical properties are well studied both in the mathematics and physics literature [23–26]; for example, their fractal dimension in $d = 2$ is $d_f = 5/4$ [22], in $d = 3$ it is $d_f \simeq 1.6236(4)$ [27, 28], while its upper critical dimension is $d_u = 4$ where $d_f = 2$ with a logarithmic correction [29]. See METHODS for further details.

Knowing the fractal dimensions of LERWs allows us to directly verify the predictions of Eqs. (3)–(5):

Volume evolution. Equation (3) predicts that the total volume of the physical network evolves as $V_t \sim t^{1-d_f/d}$. Figure 2a shows the excellent agreement between the theoretical predictions and numerical simulations. Note that, as expected, in the mean-field regime $d \geq 4$ the network volume follows the classic diffusion growth $V_t \sim t^{1/2}$. Figure 2b further corroborates the predicted scaling of the number of nodes at saturation, i.e., $N_{\text{sat}} \sim L^d$.

Degree-volume correlations. A second prediction is the emergence of volume-degree correlations, capturing the interplay between the physical layout \mathcal{P} and the combinatorial network \mathcal{G} . In particular, Eq. (4) predicts a linear proportionality between the node volume v_i and degree k_i , and we again find excellent agreement with simulations for all the tested dimensions (Fig. 2c).

Power law emergence. As a final test, we verify the emergence of power law scaling in the degree distribution of the combinatorial networks \mathcal{G} . As anticipated in Eq. (5), the degree exponent depends on both the dimensionality of the embedding substrate, d , and the fractal dimension of the LERW, d_f . Figure 2d shows that numerical simulations confirm the predicted degree exponent $\gamma = 1 + d/d_f$ for dimensions $d < 4$, while the mean-field exponent $\gamma_{\text{MF}} = 3$ is found for $d \geq 4$. In traditional models of combinatorial networks, heterogeneity typically arises from preferential attachment or some other optimization process. Our model is based on random growth without any explicit preference to create highly connected nodes; therefore, the uniform attachment tree may be considered as the non-physical counterpart of our model. Uniform attachment yields exponential degree distribution, hence the power law distribution observed here is a direct consequence of volume exclusion, which, together with the dynamic network growth, induces effective preferential attachment.

PHYSICAL NETWORK LAPLACIAN

The layout \mathcal{P} is a physical realization of the combinatorial network \mathcal{G} . Traditional studies of dynamics on physical networks ignore the layout \mathcal{P} and focus only on the role of \mathcal{G} , thus prompting the question: does modeling dynamics on \mathcal{G} accurately capture dynamics on physical networks? To explore this, we study the spectral properties of \mathcal{P} and show that physical nodes emerge as functional units through timescale separation, yet even in this limit the structure of \mathcal{P} continues to affect the dynamics. We focus on the Laplacian spectrum [12] since it influences the behavior of several dynamical processes on networks [30] including diffusion [31, 32], synchronization [33] and it underlies the definition of several information-theoretic tools to analyze the multiscale functioning of networks [10, 14, 34–37].

We study the problem by invoking, once again, the network-of-networks representation. In our setup, we assign a weight to each connection in \mathcal{P} such that links within physical nodes have weight 1 and links connecting two physical nodes have weight w , capturing that in real physical networks bonds between nodes are often qualitatively different than those within nodes. The weighted Laplacian matrix of \mathcal{P} occupying V sites is then $\mathbf{Q}_{\mathcal{P}} = \mathbf{D}_{\mathcal{P}} - \mathbf{A}_{\mathcal{P}}$, where $\mathbf{A}_{\mathcal{P}}$ is the $V \times V$ weighted adjacency matrix and $\mathbf{D}_{\mathcal{P}}$ is a diagonal matrix such that

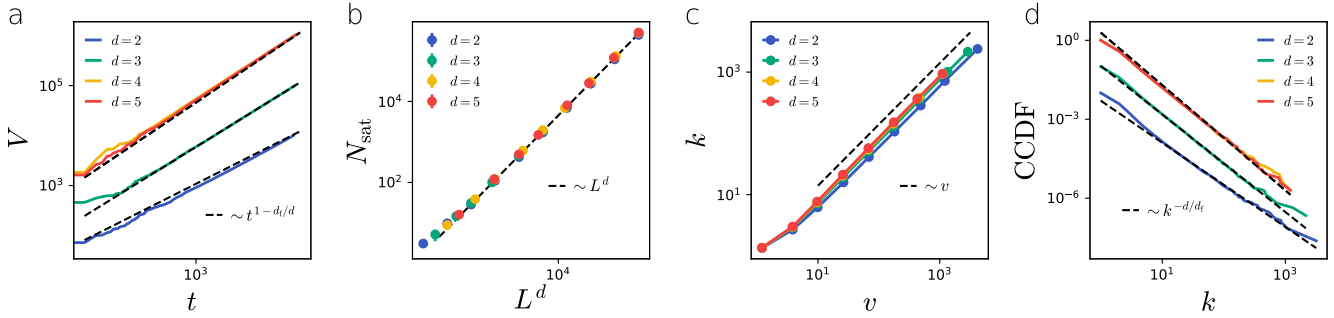


FIG. 2. **Evolution of LERW physical networks.** (a) The temporal evolution of the total volume V_i of physical networks, dashed lines represent the theoretical prediction Eq. (3). Networks built from LERWs in dimensions $d \geq 4$ fall into the mean-field regime. (b) The number of physical nodes in the saturated networks is proportional to the volume of the substrate $|\mathcal{S}|$ irrespective of d_f and d . (c) Node degree is proportional to node volume independently from d_f and d . (d) The complementary cumulative degree distribution (CCDF) of the physical networks. Dashed lines indicate the predicted degree exponent $\gamma = 1 + d/d_f \leq 3$, where $\gamma = 3$ corresponds to the mean-field behavior. Plots (a), (c) and (d) represent measurements of single networks with initial condition $v_0 = L^{d_f}$ and $|\mathcal{S}| = 10^6$. In (b) markers are an average of 10 independent networks, error bars represent the standard error of the mean. Lines corresponding to different slopes are shifted to increase readability.

$[\mathbf{D}_{\mathcal{P}}]_{ss} = \sum_u [\mathbf{A}_{\mathcal{P}}]_{su}$ is the sum of the weights of the links adjacent to site s in \mathcal{P} . If we now set $w = 0$, the network-of-networks falls apart and each physical node becomes a separate connected component, resulting in a block-diagonal Laplacian $\mathbf{Q}_{\mathcal{P}}(0) = \text{diag}(\mathbf{Q}_{\mathcal{V}_1}, \mathbf{Q}_{\mathcal{V}_2}, \dots, \mathbf{Q}_{\mathcal{V}_N})$, where $\mathbf{Q}_{\mathcal{V}_i}$ is the Laplacian of the physical node \mathcal{V}_i . The Laplacian $\mathbf{Q}_{\mathcal{P}}(0)$ has N zero eigenvalues corresponding to the N blocks (i.e., the physical nodes), hence we can assign an eigenvector $\mathbf{u}_i(w = 0)$ to the i -th node such that $[\mathbf{u}_i(0)]_s = 1/\sqrt{v_i}$ if site s is within node i , otherwise $[\mathbf{u}_i(0)]_s = 0$, where $v_i = |\mathcal{V}_i|$ is the volume of node i . Since linear combinations of these vectors are also eigenvectors, we can write the zero eigenvectors of $\mathbf{Q}_{\mathcal{P}}$ as $\mathbf{u}(0) = \mathbf{M}\tilde{\mathbf{u}}$, where \mathbf{M} is the $N \times V$ membership matrix such that $[\mathbf{M}]_{si} = 1/\sqrt{v_i}$ if site s is part of node i , otherwise $[\mathbf{M}]_{si} = 0$, and $\tilde{\mathbf{u}}$ is any normalized N dimensional vector.

We can gain insights about the spectral properties of $\mathbf{Q}_{\mathcal{P}}$ by working in the weak coupling regime $w \ll 1$ and relying on perturbation theory. Following a treatment similar to the one adopted to study diffusion in multilayer networks [38–40], we consider w a small perturbation and write $\mathbf{Q}_{\mathcal{P}}(w) = \mathbf{Q}_{\mathcal{P}}(0) + w\mathbf{Q}'_{\mathcal{P}}$, where $\mathbf{Q}'_{\mathcal{P}}$ is the Laplacian matrix of the subnetwork of \mathcal{P} formed by the bonds between physical nodes. The characteristic equation, up to first order in w , becomes then

$$\begin{aligned} \left(\mathbf{Q}_{\mathcal{P}}(0) + w\mathbf{Q}'_{\mathcal{P}}\right) \left(\mathbf{u}(0) + w\mathbf{u}'\right) &\approx \\ &\approx \left(\lambda(0) + w\lambda'\right) \left(\mathbf{u}(0) + w\mathbf{u}'\right). \end{aligned} \quad (6)$$

Perturbations around $\lambda(0) = 0$ lead to N eigenvalues that are $\mathcal{O}(w)$, while the rest of the eigenvalues are constant in leading order (Fig. 3a). This means that on the $1/w$ timescale, diffusion-like dynamics on the physical network are captured by the N slow eigenmodes. We

obtain these from Eq. (6) (see METHODS), yielding

$$\mathbf{V}^{-1/2} \mathbf{Q}_{\mathcal{G}} \mathbf{V}^{-1/2} \tilde{\mathbf{u}} = \lambda' \tilde{\mathbf{u}}, \quad (7)$$

where $\mathbf{Q}_{\mathcal{G}}$ is the $N \times N$ Laplacian matrix of the combinatorial network \mathcal{G} and \mathbf{V} is an $N \times N$ diagonal matrix such that its diagonal elements are $[\mathbf{V}]_{ii} = v_i$.

Equation (7) is a key relation for understanding the dynamics on physical networks since it allows to characterize the dynamics on \mathcal{P} on the timescale $1/w$ in a coarse-grained way: after integrating out the fast modes corresponding to eigenvalues $\lambda(w) \gg w$, the state of each physical node \mathcal{V}_i is given by a single variable, while the coupling between the nodes is provided by the combinatorial network \mathcal{G} . However, the combinatorial Laplacian $\mathbf{Q}_{\mathcal{G}}$ is not sufficient to capture the dynamics, and we must normalize $\mathbf{Q}_{\mathcal{G}}$ by the volume of the nodes, as shown in Eq. (7). This means that physical networks with the same combinatorial network but different layout can have drastically different dynamical properties. For example, if nodes have approximately the same size, i.e., $v_i \approx V/N$, then the physical layout only affects the overall timescale, otherwise the Laplacian spectrum is determined by $\mathbf{Q}_{\mathcal{G}}$. If, however, node sizes are heterogeneously distributed, normalizing by volume will also have a heterogeneous effect on the eigenvalues.

Application to the physical network growth model. We showed above that physical networks generated by our network growth model are characterized by heterogeneous node-volume distribution and a proportionality between the degree and the volume of nodes (Fig. 2). To probe the effect of this emergent correlation, we shuffle the volume of the nodes of a LERW physical network to remove the correlation between network and physical structure. We then compare the spectrum of the volume-normalized Laplacian $\mathbf{V}^{-1/2} \mathbf{Q}_{\mathcal{G}} \mathbf{V}^{-1/2}$ to its ran-

domized version $\mathbf{V}_{\text{rand}}^{-1/2} \mathbf{Q}_{\mathcal{G}} \mathbf{V}_{\text{rand}}^{-1/2}$ and to the Laplacian spectrum of the combinatorial network $\mathbf{Q}_{\mathcal{G}}$. Figure 3b shows that the spectrum of $\mathbf{Q}_{\mathcal{G}}$ has a heavy tail characterized by the same γ exponent of Eq. (5), as expected for combinatorial networks with power-law degree distributions [12]. Adding heterogeneous but uncorrelated node sizes does not influence the tail, while taking into account the degree-volume correlation of nodes removes the heavy tail and leads to a rapidly decaying spectrum. In power law networks, the eigenvector corresponding to the largest eigenvalue λ_N of $\mathbf{Q}_{\mathcal{G}}$ is typically concentrated on the node with the largest degree [41, 42]. In our model, the largest degree node also has the largest volume; therefore normalizing by node volume $\mathbf{V}^{-1/2} \mathbf{Q}_{\mathcal{G}} \mathbf{V}^{-1/2}$ significantly lowers λ_N . Since node sizes are heterogeneously distributed, with high probability we associate volume ~ 1 to the highest degree node after randomization. Hence, the eigenvalue λ_N of $\mathbf{Q}_{\mathcal{G}}$ is largely unaffected by the randomized normalization (Fig. 3c). At the other end of the spectrum, controlling the long-time mixing of the dynamics, the eigenvector associated to the algebraic connectivity λ_2 typically spans the entire network. Figure 3d shows that taking node volumes into account slows the dynamics down; however, degree-volume correlations do not significantly affect λ_2 .

Note that the number of connections a physical node can establish is bound by its volume up to a constant factor; therefore the total volume V of \mathcal{P} is bound by the number of links in \mathcal{G} from below. The saturated networks generated by our model are optimal in the sense that the network's volume reaches this lower bound asymptotically in the large L^d limit. More generally, in any optimal physical realization \mathcal{P} that reaches this lower bound, the volume of the nodes must be proportional to their degree. Therefore the Laplacian spectrum of any optimally embedded physical network has a similar volume-degree correlation as our model, hence its Laplacian spectrum is similarly affected by physicality as our model.

DISCUSSION

Physical networks, such as neural networks or three-dimensional integrated circuits, are complex networks that have a complex three-dimensional layout. Our model vividly demonstrates that traditional methods of network science focusing on combinatorial networks cannot fully describe such systems and that physical structure must be accounted for. We identified node degree and volume heterogeneity and the correlations between them as important quantities describing physical networks. These quantities are (i) shaped by volume exclusion during network evolution and (ii) have a strong effect on their functioning as captured by the physical Laplacian. The usefulness of the mathematical tools that we introduced, such as the network-of-networks repre-

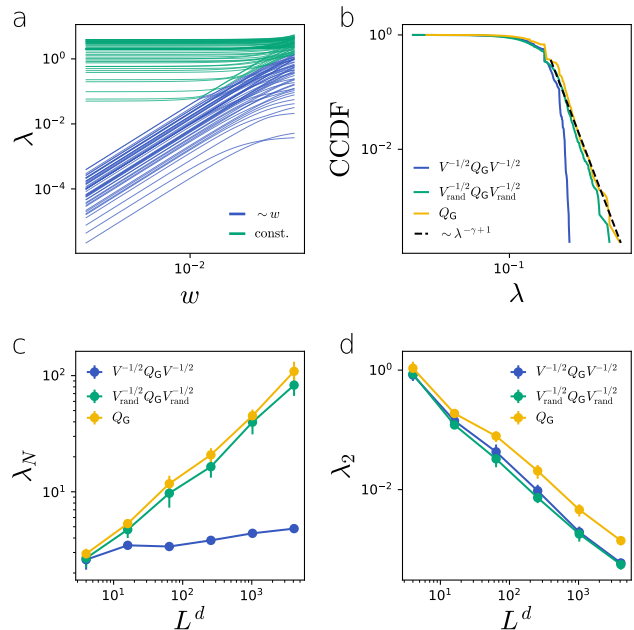


FIG. 3. Laplacian of LERW physical networks. (a) For decreasing weight w the eigenvalues of $\mathbf{Q}_{\mathcal{P}}$ separate into two groups: eigenvalues corresponding to the zero eigenmodes of $\mathbf{Q}_{\mathcal{P}}$ ($w = 0$) decay as $\sim w$ (blue), while the rest converge to a constant value (teal). (b-d) Comparing the spectrum of the volume normalized Laplacian $\mathbf{V}^{-1/2} \mathbf{Q}_{\mathcal{G}} \mathbf{V}^{-1/2}$, the randomized Laplacian $\mathbf{V}_{\text{rand}}^{-1/2} \mathbf{Q}_{\mathcal{G}} \mathbf{V}_{\text{rand}}^{-1/2}$, and the Laplacian of the combinatorial network $\mathbf{Q}_{\mathcal{G}}$. (b,c) The heterogeneous node volume distribution and the correlation between node degree and volume significantly reduce the largest eigenvalues of the spectra. (d) Heterogeneous node volumes alone explain the reduction of the algebraic connectivity λ_2 . Eigenvalues are calculated for $d = 2$ and $L = 10$ in (a) and $L = 100$ in (b). In (c) and (d) markers are an average of 10 independent networks, error bars represent the standard error of the mean.

sentation or the physical Laplacian matrix, go beyond the specifics of the model and allow us to explore the effect of physicality on real networks. Take, for example, a recently published data set describing the three-dimensional layout of more than 20,000 neurons of a fruit fly's brain and the location of more than 13 million synapses connecting them (Fig. 4a) [15]. Although we focused on model networks that are trees, the fruit fly brain is in many ways qualitatively similar to the model networks. The tail of the degree distribution can be approximated by a power law [43, 44] and we find a strong positive correlation between the degree and the volume of the nodes (Fig. 4b,c). These structural properties affect the dynamics on the brain network similarly to what we observed for model networks: the Laplacian spectrum of the combinatorial network inherits the heterogeneity of the degree distribution. If, however, we take into account physicality, i.e., we normalize the Laplacian matrix by the node volumes, the power law tail of the spectrum

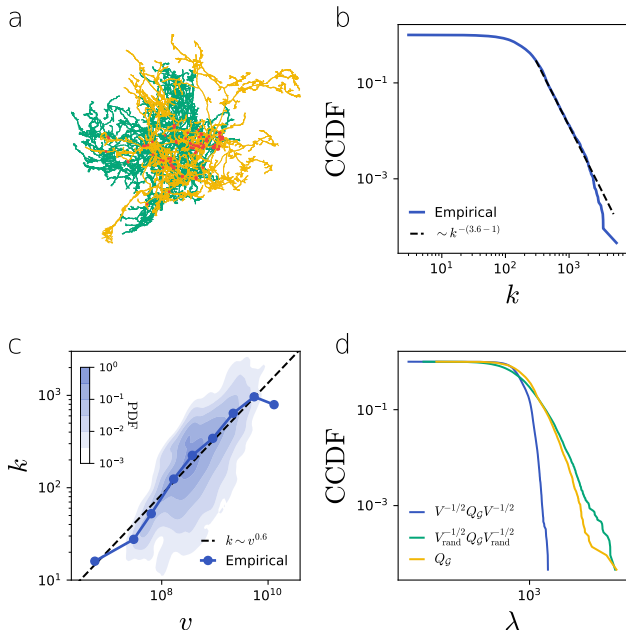


FIG. 4. **Fruit fly brain network.** (a) The neurons have complex three-dimensional shapes. Two intertwined neurons (teal and yellow) are connected by synapses (red circles). (b) The tail of the degree distribution can be approximated with the power law with $\gamma_{\text{ff}} \approx 3.6$. (c) Similar to the network growth model, the volume of the nodes v is strongly correlated with their degree k ; however, the relationship between v and k is sub-linear. Circles indicate binned averages, shading represents a kernel density estimate of the joint v - k distribution. (d) The effect of the node volume-degree correlation on the Laplacian spectrum in the brain network is analog to the effect of correlations in the network growth model.

is suppressed due to the correlation between node degree and volume. There are differences, however, that the model is unable to capture; for example, the degree exponent of the brain network is $\gamma_{\text{ff}} \approx 3.6$ and the relationship between node volume and degree is sub-linear, while the degree exponent of the model is always $\gamma \leq 3$ and the relation between degree and size is linear $k \sim v$. Future work may aim to understand the origin of these features, for example, by allowing nodes to branch and create multiple connections or introducing additional interactions between nodes.

MATERIALS AND METHODS.

Loop-erased random walks. In our network growth model, we can generate physical nodes with any stochastic or deterministic process that produces a growing fractal embedded in \mathbb{Z}^d . Standard self-avoiding walks are traditionally used to model polymers obeying volume exclusion, and therefore represent a natural choice to model node growth [17]. However, the naïve kinetic version of the self-avoiding walk traps itself in two and three dimensions at finite length [21], making it a poor candidate to construct large physical networks. Instead, we focus on loop-erased random walks (LERW): a LERW evolves as a simple random walk, except when it intersects itself, we delete the loop that it created and continue the walk [20]. This guarantees that the final physical node does not intersect itself and that the walk never gets trapped. Alternatively, the LERW can be defined as special case of Laplacian-random walks, where transition probabilities are defined by a harmonic function [45, 46]. This alternative construction does not require deleting loops, hence is more realistic as a growth model. The LERW has attractive mathematical properties making it amenable to analytical treatment. For example, Wilson’s algorithm uses iterative LERWs to construct a uniform spanning tree (UST) of any graph [24]. In fact, the physical network our algorithm constructs is a UST of the \mathcal{S} substrate together with a partition identifying the nodes. Future work may exploit this connection between USTs and LERW physical networks, together with known results in dimensions $d = 2$ and $d > 4$ dimensions [47, 48], to rigorously prove some of the results presented here.

Perturbation of the physical Laplacian. To obtain the slow eigenmodes, we match the first order terms of Eq. (6) and substitute $\mathbf{u}(0) = \mathbf{M}\tilde{\mathbf{u}}$, so that

$$\mathbf{Q}_{\mathcal{P}}(0)\mathbf{u}' + \mathbf{Q}'_{\mathcal{P}}\mathbf{M}\tilde{\mathbf{u}} = \lambda'\mathbf{M}\tilde{\mathbf{u}}. \quad (8)$$

Multiplying from the left by the transpose of the membership matrix \mathbf{M} we get

$$\mathbf{M}^T\mathbf{Q}_{\mathcal{P}}(0)\mathbf{u}' + \mathbf{M}^T\mathbf{Q}'_{\mathcal{P}}\mathbf{M}\tilde{\mathbf{u}} = \lambda'\mathbf{M}^T\mathbf{M}\tilde{\mathbf{u}}. \quad (9)$$

The i th row of \mathbf{M}^T is the trivial eigenvector $\mathbf{u}_i(w = 0)$ corresponding to physical node i ; therefore $\mathbf{M}^T\mathbf{Q}_{\mathcal{P}}(0)$ is all zeros and $\mathbf{M}^T\mathbf{M}$ is the $N \times N$ identity matrix, leading to Eq. (7) in the text.

The fruit fly connectome. This data set describes a portion of the central brain of the fruit fly, *Drosophila melanogaster* [15]. The physical layout of the connectome is provided by the detailed three dimensional shape of each neuron and the location of the synapses between them. The corresponding combinatorial network contains 21,662 nodes representing neurons and 13,603,750 links representing synapses. Synaptic partners are connected through approximately 5 synapses on average, and the maximum number of synapses between two neurons

is 6039. In our calculations, we treat the combinatorial network as a weighted and undirected network. Note that we only require the combinatorial network and the volume of each node for our calculations; therefore the detailed physical layout of the connectome is in fact not needed.

We find that the weighted degree distribution has a heavy tail, which can be approximated by a power law with $\gamma_{\text{ff}} \approx 3.6$ for degrees ≥ 448 ; the power law fit, however, cannot be distinguished from a lognormal fit on the same range [43, 44]. To calculate the spectrum of the physical Laplacian, we normalize the node volume by its minimum value.

Acknowledgments. IB and MP were funded by ERC grant No. 810115-DYNASET. AT and SÖS acknowledge partial support from the Icelandic Research Fund, grant No. 239736-051. GP was funded by the ERC Consolidator Grant No.-772466 “NOISE”.

* posfaim@ceu.edu

- [1] N. Dehmamy, S. Milanlouei, and A.-L. Barabási. A structural transition in physical networks. *Nature*, 563(7733):676–680, 2018.
- [2] Y. Liu, N. Dehmamy, and A.-L. Barabási. Isotopy and energy of physical networks. *Nature Physics*, 17(2):216–222, 2021.
- [3] M. Pósfai, B. Szegedy, I. Bačić, L. Blagojević, M. Abért, J. Kertész, L. Lovász, and A.-L. Barabási. Understanding the impact of physicality on network structure. *arXiv preprint arXiv:2211.13265*, 2022.
- [4] E. Bullmore and O. Sporns. Complex brain networks: graph theoretical analysis of structural and functional systems. *Nature Reviews Neuroscience*, 10(3):186–198, 2009.
- [5] M. P. Viana, A. I. Brown, I. A. Mueller, C. Goul, E. F. Koslover, and S. M. Rafelski. Mitochondrial fission and fusion dynamics generate efficient, robust, and evenly distributed network topologies in budding yeast cells. *Cell systems*, 10(3):287–297, 2020.
- [6] D. A. Fletcher and R. D. Mullins. Cell mechanics and the cytoskeleton. *Nature*, 463(7280):485–492, 2010.
- [7] Catalin R Picu. Network materials: Structure and properties. 2022.
- [8] S. W Simard, D. A. Perry, M. D. Jones, D. D. Myrold, D. M. Durall, and R. Molina. Net transfer of carbon between ectomycorrhizal tree species in the field. *Nature*, 388(6642):579–582, 1997.
- [9] B. S. Steidinger, T. W. Crowther, J. Liang, M. E. Van Nuland, G. D. A. Werner, P. B. Reich, G.-J. Nabuurs, S. de Miguel, M. Zhou, N. Picard, et al. Climatic controls of decomposition drive the global biogeography of forest-tree symbioses. *Nature*, 569(7756):404–408, 2019.
- [10] M. De Domenico, A. Solé-Ribalta, E. Cozzo, M. Kivela, Y. Moreno, M. A. Porter, S. Gómez, and A. Arenas. Mathematical formulation of multilayer networks. *Physical Review X*, 3(4):041022, 2013.
- [11] G. Bianconi. *Multilayer networks: structure and function*. Oxford university press, 2018.
- [12] P. Van Mieghem. *Graph spectra for complex networks*. Cambridge University Press, 2010.
- [13] C. Castellano and R. Pastor-Satorras. Relating topological determinants of complex networks to their spectral properties: Structural and dynamical effects. *Physical Review X*, 7(4):041024, 2017.
- [14] P. Villegas, T. Gili, G. Caldarelli, and A. Gabrielli. Laplacian renormalization group for heterogeneous networks. *Nature Physics*, pages 1–6, 2023.
- [15] L. K. et al. Scheffer. A connectome and analysis of the adult drosophila central brain. *Elife*, 9:e57443, 2020.
- [16] R. Tamassia. *Handbook of graph drawing and visualization*. CRC press, 2013.
- [17] T. Vicsek. *Fractal growth phenomena*. World scientific, 1992.
- [18] A. Bunde and S. Havlin. *Fractals and disordered systems*. Springer Science & Business Media, 2012.
- [19] P.-G. de Gennes. Exponents for the excluded volume problem as derived by the wilson method. *Phys. Lett. A*, 38(5):339–340, 1972.
- [20] G. F. Lawler. A self-avoiding random walk. 1980.
- [21] L. Pietronero. Survival probability for kinetic self-avoiding walks. *Phys. Rev. Lett.*, 55(19):2025, 1985.
- [22] O. Schramm. Scaling limits of loop-erased random walks and uniform spanning trees. In *Selected Works of Oded Schramm*, pages 791–858. Springer, 2011.
- [23] L. Niemeyer, L. Pietronero, and H. J. Wiesmann. Fractal dimension of dielectric breakdown. *Phys. Rev. Lett.*, 52(12):1033, 1984.
- [24] D. B. Wilson. Generating random spanning trees more quickly than the cover time. In *Proceed. of the 28th ACM Theory of computing*, pages 296–303, 1996.
- [25] G. F. Lawler, O. Schramm, and W. Werner. Conformal invariance of planar loop-erased random walks and uniform spanning trees. In *Selected Works of Oded Schramm*, pages 931–987. Springer, 2011.
- [26] K. Wiese and A. A. Fedorenko. Field theories for loop-erased random walks. *Nuclear Physics B*, 946:114696, 2019.
- [27] H. Agrawal and D. Dhar. Distribution of sizes of erased loops of loop-erased random walks in two and three dimensions. *Phys. Rev. E*, 63(5):056115, 2001.
- [28] P. Grassberger. Scaling of loop-erased walks in 2 to 4 dimensions. *Journal of statistical physics*, 136:399–404, 2009.
- [29] D. B. Wilson. Dimension of the loop-erased random walk in three dimensions. *Phys. Rev. E*, 82(6):062102, 2010.
- [30] A. Barrat, M. Barthelemy, and A. Vespignani. *Dynamical processes on complex networks*. Cambridge University Press, 2008.
- [31] N. Masuda, M. A. Porter, and R. Lambiotte. Random walks and diffusion on networks. *Phys. Rep.*, 716:1–58, 2017.
- [32] M. De Domenico and J. Biamonte. Spectral entropies as information-theoretic tools for complex network comparison. *Phys. Rev. X*, 6(4):041062, 2016.
- [33] A. Arenas, A. Díaz-Guilera, J. Kurths, Y. Moreno, and C. Zhou. Synchronization in complex networks. *Phys. Rep.*, 469(3):93–153, 2008.
- [34] Marian Boguna, Ivan Bonamassa, Manlio De Domenico, Shlomo Havlin, Dmitri Krioukov, and M Ángeles Serrano. Network geometry. *Nature Reviews Physics*, 3(2):114–135, 2021.

- [35] Arsham Ghavasieh, Massimo Stella, Jacob Biamonte, and Manlio De Domenico. Unraveling the effects of multiscale network entanglement on empirical systems. *Communications Physics*, 4(1):129, 2021.
- [36] P. Villegas, A. Gabrielli, F. Santucci, G. Caldarelli, and T. Gili. Laplacian paths in complex networks: Information core emerges from entropic transitions. *Phys. Rev. Res.*, 4(3):033196, 2022.
- [37] Arsham Ghavasieh and Manlio De Domenico. Generalized network density matrices for analysis of multiscale functional diversity. *Physical Review E*, 107(4):044304, 2023.
- [38] S. Gomez, A. Diaz-Guilera, J. Gomez-Gardenes, C. J. Perez-Vicente, Y. Moreno, and A. Arenas. Diffusion dynamics on multiplex networks. *Phys. Rev. Lett.*, 110(2):028701, 2013.
- [39] A. Sole-Ribalta, M. De Domenico, N. E. Kouvaris, A. Diaz-Guilera, S Gomez, and A. Arenas. Spectral properties of the laplacian of multiplex networks. *Physical Review E*, 88(3):032807, 2013.
- [40] F. Radicchi and A. Arenas. Abrupt transition in the structural formation of interconnected networks. *Nature Physics*, 9(11):717–720, 2013.
- [41] R. Pastor-Satorras and C. Castellano. Distinct types of eigenvector localization in networks. *Sci. Rep.*, 6(1):18847, 2016.
- [42] S. Hata and H. Nakao. Localization of laplacian eigenvectors on random networks. *Sci. Rep.*, 7(1):1–11, 2017.
- [43] Aaron Clauset, Cosma Rohilla Shalizi, and Mark EJ Newman. Power-law distributions in empirical data. *SIAM review*, 51(4):661–703, 2009.
- [44] Jeff Alstott, Ed Bullmore, and Dietmar Plenz. powerlaw: a python package for analysis of heavy-tailed distributions. *PLoS one*, 9(1):e85777, 2014.
- [45] J. W. Lyklema, C. Evertsz, and L. Pietronero. The laplacian random walk. *EPL (Europhysics Letters)*, 2(2):77, 1986.
- [46] G. F. Lawler. Loop-erased self-avoiding random walk and the laplacian random walk. *Journal of Physics A: Mathematical and General*, 20(13):4565, 1987.
- [47] O. Schramm. Scaling limits of loop-erased random walks and uniform spanning trees. *Israel Journal of Mathematics*, 118(1):221–288, 2000.
- [48] S. Bhupatiraju, J. Hanson, and A. A. Járai. Inequalities for critical exponents in d-dimensional sandpiles. 2017.